

## Natural Product Micheliolide (MCL) Irreversibly Activates Pyruvate Kinase M2 and Suppresses Leukemia

Jing Li,<sup>†</sup> Shanshan Li,<sup>‡</sup> Jianshuang Guo,<sup>†</sup> Qiuying Li,<sup>†</sup> Jing Long,<sup>†</sup> Cheng Ma,<sup>‡</sup> Yahui Ding,<sup>†</sup> Chunli Yan,<sup>‡</sup> Liangwei Li,<sup>‡</sup> Zhigang Wu,<sup>‡</sup> He Zhu,<sup>‡</sup> Keqin Kathy Li,<sup>‡</sup> Liuqing Wen,<sup>‡</sup> Quan Zhang,<sup>†</sup> Qingqing Xue,<sup>†</sup> Caili Zhao,<sup>†</sup> Ning Liu,<sup>†</sup> Ivaylo Ivanov,<sup>‡</sup> Ming Luo,<sup>‡</sup> Rimo Xi,<sup>†</sup> Haibo Long,<sup>§</sup> Peng George Wang,<sup>\*,†,‡</sup> and Yue Chen<sup>\*,†</sup>

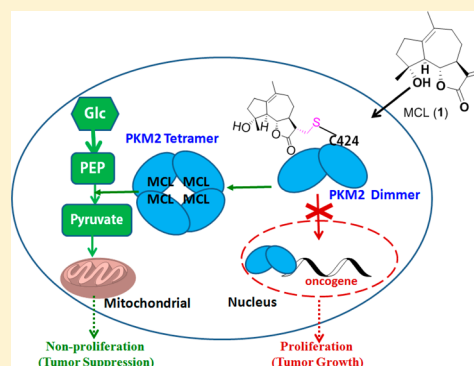
<sup>†</sup>State Key Laboratory of Medicinal Chemical Biology, College of Pharmacy and Tianjin Key Laboratory of Molecular Drug Research, Nankai University, Haihe Education Park, 38 Tongyan Road, Tianjin 300350, China

<sup>‡</sup>Center for Diagnostics and Therapeutics, Department of Chemistry, Georgia State University, Atlanta, Georgia 30303, United States

<sup>§</sup>Department of Nephrology, Zhujiang Hospital, Southern Medical University, Guangzhou 510280, China

### Supporting Information

**ABSTRACT:** Metabolic reprogramming of cancer cells is essential for tumorigenesis in which pyruvate kinase M2 (PKM2), the low activity isoform of pyruvate kinase, plays a critical role. Herein, we describe the identification of a nature-product-derived micheliolide (MCL) that selectively activates PKM2 through the covalent binding at residue cysteine424 (C424), which is not contained in PKM1. This interaction promotes more tetramer formation, inhibits the lysine433 (K433) acetylation, and influences the translocation of PKM2 into the nucleus. In addition, the pro-drug dimethylaminomicheliolide (DMAMCL) with similar properties as MCL significantly suppresses the growth of leukemia cells and tumorigenesis in a zebrafish xenograft model. Cell-based assay with knock down PKM2 expression verifies that the effects of MCL are dependent on PKM2 expression. DMAMCL is currently in clinical trials in Australia. Our discovery may provide a valuable pharmacological mechanism for clinical treatment and benefit the development of new anticancer agents.



## INTRODUCTION

Metabolic reprogramming toward aerobic glycolysis is a critical hallmark of cancers, enabling cancer cells to obtain more biosynthetic materials for the growth and division of rapidly proliferating cells.<sup>1</sup> Pyruvate kinases, which catalyze the conversion of phosphoenol-pyruvate (PEP) to pyruvate at the final step of glycolysis, have been shown to be crucial in the regulation of cancer metabolic reprogramming.<sup>2,3</sup> Multiple lines of evidence have indicated that the M2 isoform of pyruvate kinase (PKM2) is upregulated in most cancer cells and tumors tested so far.<sup>1</sup> In contrast to its splice variant PKM1, which is expressed in normal differentiated tissues as a stable tetramer, PKM2 exists in equilibrium among monomer, dimer, and tetramer forms, which was regulated by the allosteric binding of metabolic effectors or post-translational modifications (Figure 1A).<sup>2–4</sup> These different catalytic and regulatory properties are all ascribed to 22 distinct amino acids between PKM1 and PKM2 (Figure 1B).<sup>1</sup> In cancer cells, more negative allosteric modulations, including phosphor-tyrosine and numerous post-translational modifications, cause the PKM2 tetramer to dissociate into a dimeric formation. Dimeric PKM2 is much less active, and its presence diverts the glycolytic flux to increased biomass production, contributing to oncogenesis.<sup>5,6</sup> In addition, dimeric PKM2 has the potential to translocate into

the nucleus to act as transcriptional regulators of genes that promote tumorigenesis and migration.<sup>5–8</sup> Consequently, much effort has focused on the discovery and development of small-molecule PKM2 activators to promote tetramer formation or initiate its activity.<sup>9,10</sup> Herein, we describe a novel natural-product-derived PKM2 activator that shows promising efficacy for leukemia treatment and has entered clinical trials.

Sesquiterpene lactones (SLs) are a class of natural products with varied biological and pharmacological activities, including the common incorporation of trans- or cis-fused  $\gamma$ -lactone containing an  $\alpha$ -methylene group.<sup>11</sup> Parthenolide (PTL), an SL isolated from feverfew (*Tanacetum parthenium* L.), reportedly inhibits the proliferation of various human cancer cells *in vitro*.<sup>12,13</sup> However, PTL's lack of stability under both acidic and basic conditions, coupled with poor solubility, has severely limited its medicinal applications.<sup>14</sup> In our previous work, we identified micheliolide (MCL), a more stable guaianolide SL (GSL) (Figure 1C), as a new potent lead compound for reducing the proportion of acute myelogenous leukemia (AML) cells and glioma cells.<sup>15,16</sup> Most strikingly, dimethylaminomicheliolide (DMAMCL, i.e., ACT001), the pro-drug of

Received: February 12, 2018

Published: April 11, 2018

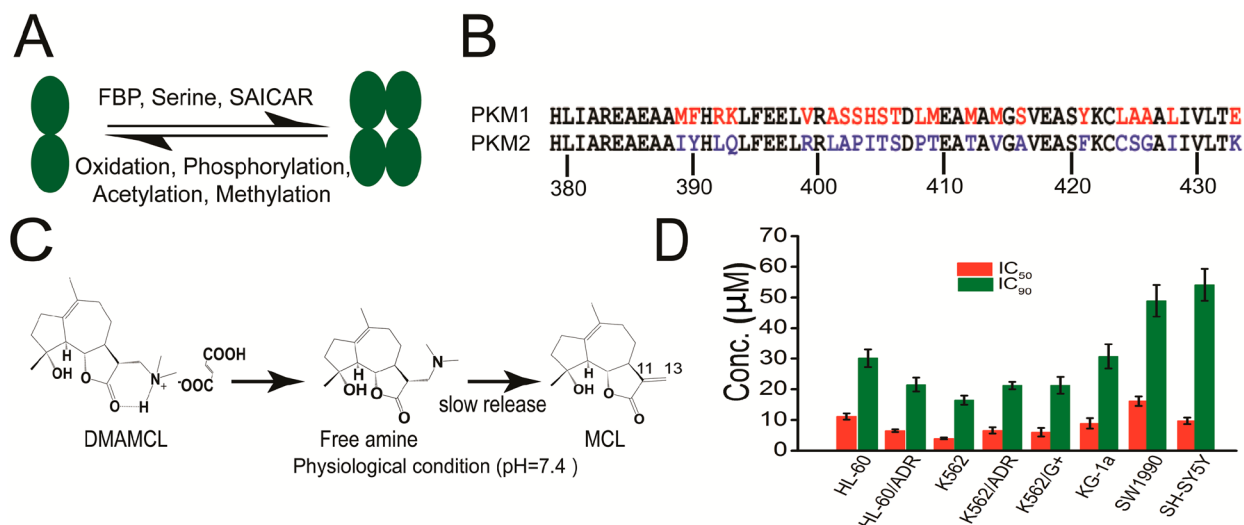


**Figure 1.** MCL is a novel allosteric activator of PKM2. (A) Allosteric regulations of PKM2. (B) Splice variant amino acids between PKM1 and PKM2. The 22 distinct amino acids are marked in red for PKM1 and in blue for PKM2. (C) Mechanism of sustainable release of MCL by DMAMCL under neutral conditions. (D) Inhibition profile of cancer cell lines by DMAMCL. Eight cancer cell lines were incubated with different concentrations of DMAMCL for 48 h. Cell proliferation was determined by MTT assay. Graphs depict mean  $\pm$  SEM from six independent experiments.

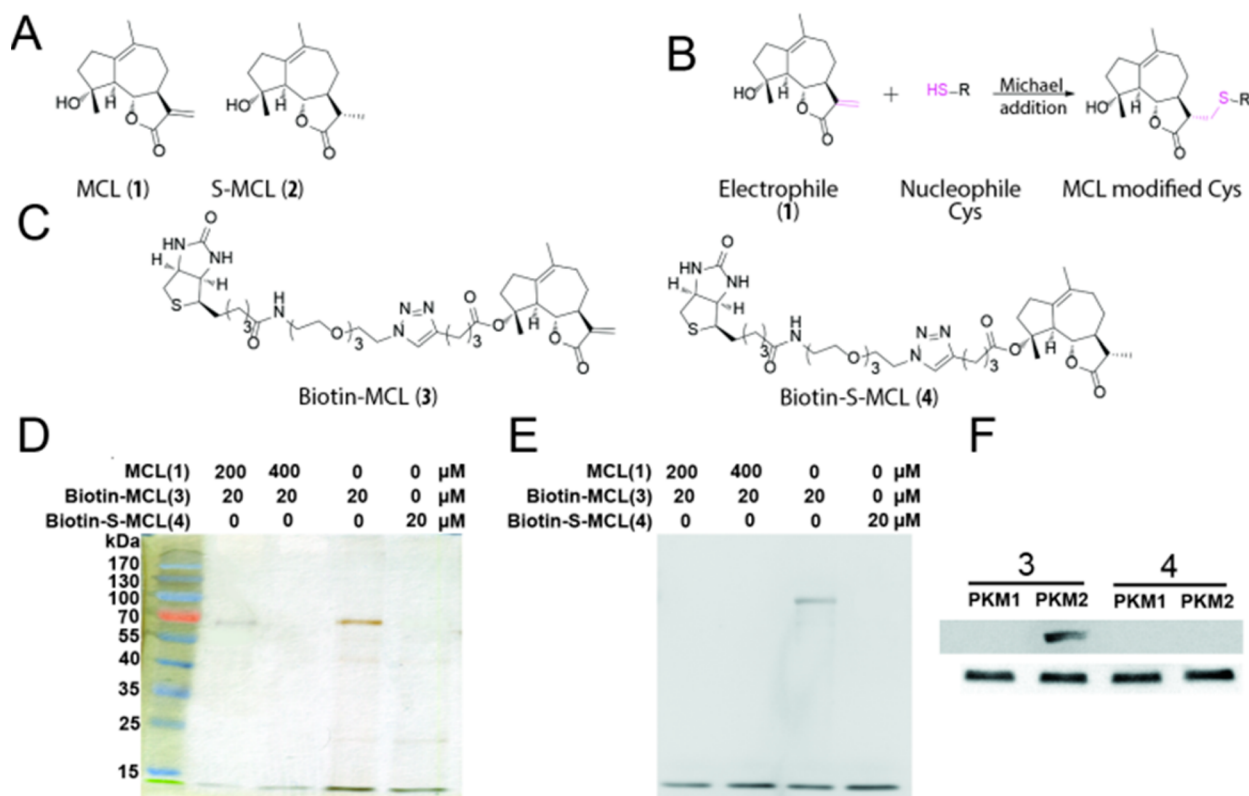


**Figure 2.** MCL directly binds to PKM2. (A) Structures of MCL (1, active) and S-MCL (2, inactive). (B) Michael addition mechanism of MCL and cysteine. (C) Structure of biotin-MCL (3, active) and biotin-S-MCL (4, inactive). (D) Silver staining of the pull-down fraction. HL60 cell lysates were incubated with 3 and 4 at 4 °C overnight. For the treatment of 3, a high concentration of MCL was added to the coinubation. The lysates were used for streptavidin-agarose pull-down assays, and the precipitates were resolved by SDS-PAGE, followed by silver staining. (E) Western blot with the same sample as in silver staining but developed by anti-PKM2. (F) Western blot detection of the binding abilities of 3 and 4 with recombinant proteins PKM1 and PKM2, respectively. rPKM1 and rPKM2 were incubated with probe 3 or 4 at 4 °C overnight. The mixture was then subjected to Western blot with streptavidin-HRP to detect the biotin-conjugated complex (top). The same sample was developed with anti-PKM1/PKM2 antibody (bottom) to show the sample amount. All experiments were repeated at least three times, with similar results.

MCL, can release MCL slowly under physiological conditions<sup>16</sup> and was recently approved for clinical trials in Australia (trial

ID: ACTRN12616000228482). However, the pharmacodynamic markers and cellular mechanism of DMAMCL remain

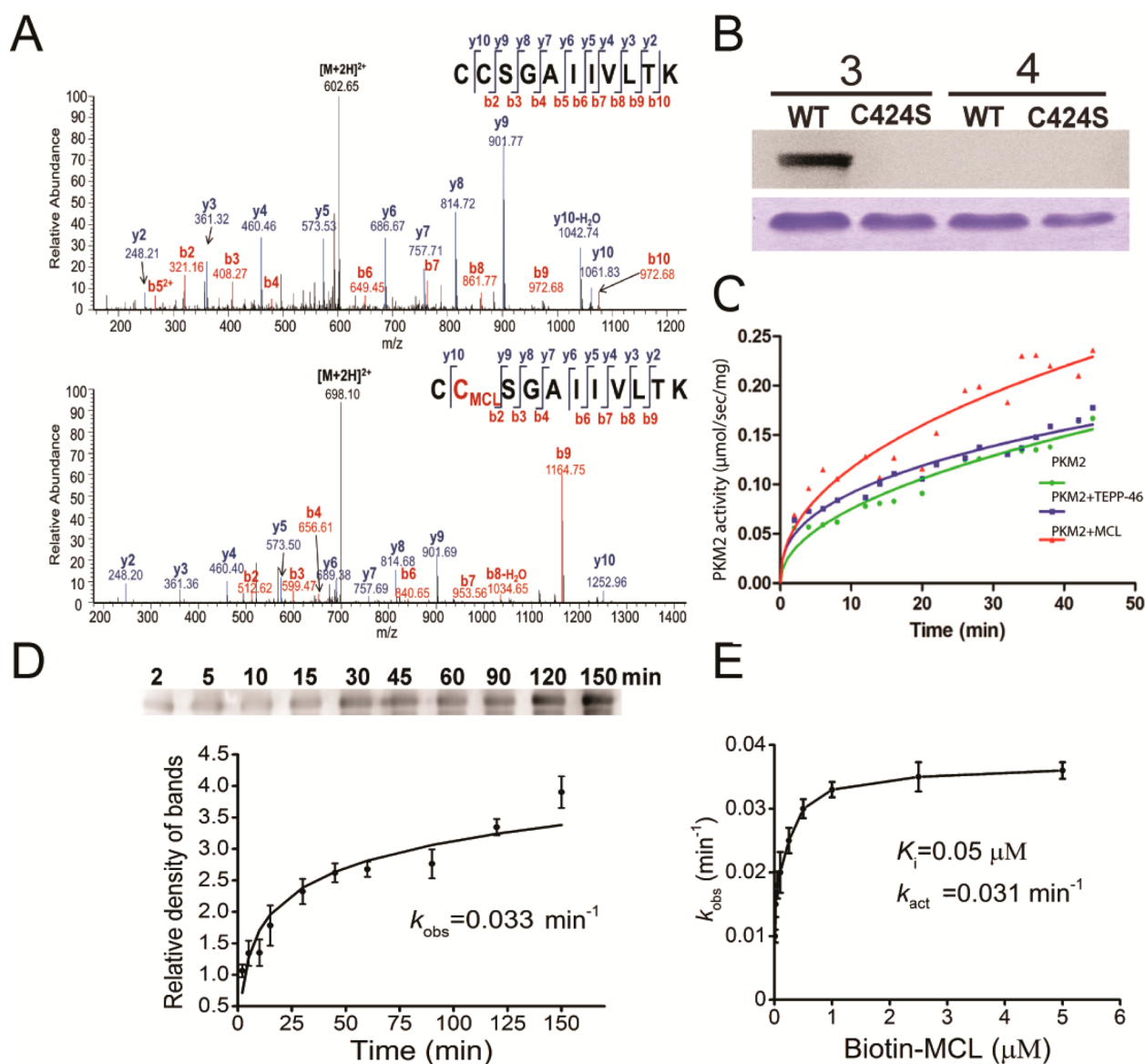


**Figure 3.** MCL targets C424 of PKM2 and activates its pyruvate kinase activity. (A) MS/MS analysis of the C424-containing tryptic peptide for rPKM2 incubated without (top) and with (bottom) MCL for 60 min at RT. C in red color represents the cysteine bound by MCL. (B) Recombinant WT PKM2 and its mutant (C424S) incubated with biotin-MCL for 60 min at RT, followed by SDS-PAGE (bottom) and Western blot to detect biotin (top). (C) Recombinant PKM2 proteins were incubated with MCL and TEPP-46 at 4 μM for 50 min at RT, and their pyruvate kinase activity was monitored over 40 min. (D) Determination of  $K_{obs}$  for the interaction of PKM2 (0.25 μM) with biotin-MCL (20 μM) for different periods of time, as described in the [Supplementary Methods](#). (E) Plotting the  $K_{obs}$  values for the binding of PKM2 as a function of MCL at different concentrations.

unknown, making their identification crucial for clinical treatment and designing more effective treatments.

In the present work, we determined that MCL is a novel natural-product-derived, covalent, and selective activator of PKM2 via binding to the conserved cysteine424 (C424) residue of PKM2, but not PKM1. This binding induces the irreversible tetramerization of PKM2, which is essential for high pyruvate kinase activity. Concomitantly, this allosteric regulation decreases lysine433 (K433) acetylation of PKM2 and lowers PKM2 nucleus translocation, which is vital for its nonmetabolic function in cell proliferation and tumorigenesis. Combined with the proliferation inhibition of several cancer cell lines and the repression of leukemia *in vivo*, DMAMCL represents the first natural lead compound for the development

of PKM2-targeted therapeutic agents to enter clinical development.

## RESULTS AND DISCUSSION

**Micheliolide Derivative DMAMCL Inhibits Multiple Cancer Cells *In Vitro*.** Our previous work has demonstrated that MCL is a potent inhibitor of AML cells<sup>16</sup> and glioma cells.<sup>15</sup> To increase the bioavailability of MCL, we also synthesized the dimethylamino Michael adduct of MCL (DMAMCL),<sup>16</sup> which exhibited high stability, lower toxicity, and sustainable release of MCL, under physiological or neutral conditions (Figure 1C). Here, a wide range of cancer cell lines, including drug-resistant and sensitive leukemia cell lines (HL-60, K562, and KG-1a), a human pancreatic adenocarcinoma cell line (SW1990), and a human neuroblastoma cell line (SH-



SY5Y), HL60 were treated with DMAMCL and assayed for the cell viability by MTT (3-[4,5-dimethylthiazol-2-yl]-2,5-diphenyl tetrazolium). Cell growth was inhibited in all treated cancer cell lines ( $IC_{50}$ , 3.9–16.2  $\mu\text{M}$ ;  $IC_{90}$ , 16.4–54.14  $\mu\text{M}$ ) in a concentration-dependent manner (Figures 1D and S1). Consistent with our previous studies, the leukemia cell lines were found to be more sensitive to DMAMCL, with an  $IC_{50}$  of less than 12  $\mu\text{M}$ .<sup>16</sup>

**MCL Specifically Targets PKM2, not PKM1.** To investigate the functional target of MCL (1) that is responsible for its anticancer activity, we prepared biotin-conjugated probes for affinity purification. Our preliminary structure–activity relationship (SAR) study revealed that when the 11,13-double bond of MCL was reduced to a single bond to produce S-MCL (2) (Figure 2A), the inhibitory activity of MCL against leukemia cells was completely abolished, even at a higher concentration (10  $\mu\text{M}$ ).<sup>16</sup> These data indicate that the 11,13-double bond of MCL (1) is crucial for its anticancer activity, most likely acting as a reactive Michael acceptor and forming a covalent bond with the cysteine residues of its target protein (Figure 2B). In contrast, MCL with slight modification to its C-region largely maintained its activity against AML cells at a level comparable to that of MCL.<sup>16</sup> Thus, we incorporated a biotin tag in the C-domain of MCL (1) and its inactive analogue S-MCL (2) to yield a positive probe (3, biotin-MCL) and a negative probe (4, biotin-S-MCL) respectively (Figure 2C and Scheme S1).

Next, HL60 cell lysates were incubated with positive (3) and negative (4) probes, and the mixtures were separately pulled down with streptavidin-coated agarose beads, followed by gel electrophoresis and silver staining. A single band with a molecular mass of  $\sim 60$  kDa was clearly precipitated by 3 but not by 4 (Figure 2D). In addition, this band could be suppressed by a high concentration of MCL. Peptide mass fingerprinting data analysis identified the MCL-bound protein was PKM2 (Figure S2). Using immunoblotting, we also observed the presence of PKM2 in the precipitates (Figure 2E). To verify the selectivity of this binding, we expressed recombinant PKM2 (rPKM2) and PKM1 (rPKM1) *in vitro* and incubated them with positive (3) and negative (4) probes, respectively. The positive probe (3) effectively bound to rPKM2 but not rPKM1 (Figure 2F), further supporting the notion that PKM2, not PKM1, is the direct target of MCL.

**C424 of PKM2 Is Critical for Binding to MCL.** The 11,13-double bond of MCL (1) is a reactive Michael acceptor, we speculated that some conserved cysteine residues in PKM2 are the binding sites of MCL. To identify the specific residues modified by MCL, we incubated the rPKM2 protein with or without MCL. After the reaction, the rPKM2 protein was digested with trypsin and then analyzed by LC–MS/MS. The mass of the Cys424-containing peptide CCSGAIIVLTK was measured as 1220.626 Da in the absence of MCL and 1411.745 Da in the presence of MCL. The calculated mass shift of 191.120 Da is consistent with the addition of one molecular unit of MCL. MS/MS analyses of both unmodified and modified C424-containing peptides provided a partial series of  $\gamma$ -ion fragments corresponding to the peptide sequence. Both MS/MS spectra had the same mass from  $\gamma_2$  to  $\gamma_9$ , whereas the mass shifted by 191.120 Da for the C424-containing fragment (from  $\gamma_{10}$ ) in the spectra of the modified peptide (Figure 3A). Interestingly, C424 is located at the C–C interface of two dimers, which can affect subunit interaction, enzymatic activity, or both.<sup>17</sup> To confirm that C424 residue was the only modified

site of MCL, rPKM2 and mutant rPKM2-C424S were further expressed and incubated with biotin-MCL (3) or inactive biotin-MCL (4) and detected by Western blot. In contrast to rPKM2-C424, only rPKM2 incubated with biotin-MCL (3) produced a signal with anti-biotin, supporting our conclusion that MCL selectively binds to PKM2 at the C424 site (Figure 3B).

#### MCL Activates the Pyruvate Kinase Activity of PKM2.

To determine the effect of MCL on PKM2 activity, we measured the pyruvate kinase activity of rPKM2 proteins in the presence or absence of MCL with TEPP-46 as positive control. The results demonstrated that MCL effectively promoted the pyruvate kinase activity of rPKM2 with half-maximum activating concentration ( $AC_{50}$ ) at 6 nM, which was better than TEPP-46 ( $AC_{50}$  = 92 nM) (Figures 3C and S3). The potent activation of MCL may be due to the covalent binding of MCL, which irreversibly activates PKM2 with a cumulative effect. However, the action mode of TEPP-46 is reversible and dependent on the availability of FBP.<sup>9</sup>

To test if MCL binds to PKM2 through an irreversible covalent modification, we next assessed this binding at certain time points for several biotin-MCL concentrations. The profile of PKM2 binding with biotin-MCL at various concentrations revealed a time-dependent saturation (Figure 3D), consistent with an irreversible modification mechanism.<sup>18</sup> The data were fit to determine the observed rate constants for binding ( $K_{obs}$ ) at each concentration. Plotting the  $K_{obs}$  values as a function of the biotin-MCL (3) concentration revealed a saturation curve (Figure 3E). These data support a two-step reaction for the activation of PKM2 by MCL (1) that involves the noncovalent reversible binding of PKM2 to biotin-MCL (initial binding step,  $K_i$ ), which places the moderately reactive electrophile of MCL (1) close to a specific nucleophile on the protein, followed by a second step that results in a specific covalent linkage ( $k_{act}$ ). Based on this model, the  $k_{act}$  value for PKM2 binding with biotin-MCL (3) was calculated to be  $0.031 \text{ min}^{-1}$  (Figure 3E), suggesting a high specific reactivity, and the  $K_i$  value was 0.05  $\mu\text{M}$  (Figure 3E), indicating a high affinity. Overall, the efficiency of the binding of MCL to PKM2 was high ( $k_{act}/K_i = 1.03 \times 10^4 \text{ M}^{-1} \text{ s}^{-1}$ ), demonstrating that MCL (1) is a potent irreversible activator of PKM2.

**MCL Promotes Increased Tetramer Formation of PKM2 in Vitro or in Cells.** Tetrameric PKM2 is the only form with high pyruvate kinase activity. We next evaluated whether the activation of MCL is accompanied by the tetramerization of PKM2. Size-exclusion chromatography analysis and fraction detection by SDS-PAGE were performed on rPKM2 and MCL-treated rPKM2. Chromatography of rPKM2 indicated that rPKM2 contained a mixed population of configurations (i.e., monomers, dimers, and tetramers), with a tendency to tetramerize at higher concentrations (Figure S4A). Thus, a low concentration of rPKM2 (0.3 mg/mL), with a higher population of monomers, was used to detect the allosteric effect of MCL. As expected, the incubation of rPKM2 with 10  $\mu\text{M}$  MCL resulted in a significant shift toward a tetrameric configuration (Figure S4B,C).

Large existing phosphotyrosine (pTyr) proteins in cancer cells can bind PKM2 and catalyze the release of FBP from the enzyme.<sup>19</sup> To verify the same promotion effect of MCL on endogenous PKM2, we cultured leukemia HL60 cells treated with DMSO, MCL, pervanadate (a tyrosine phosphatase inhibitor, which can increase the amount of pTyr proteins), and pervanadate combined with MCL. The cellular proteins

including endogenous PKM2 were then extracted, normalized, and analyzed by the same chromatographic method. According to tetramer and monomer formation of PKM2, different fractions were collected and detected by Western blot with anti-PKM2 antibody. Compared to DMSO treatment, PKM2 with only pervanadate treatment appeared primarily as a dimer. In contrast, MCL treatment increased tetramer formation of PKM2, regardless of the presence or absence of pTyr. These data indicate that MCL acts as a potent tetramer inducer of PKM2 and cannot be competed-out by pTyr, even after treating the cells with pervanadate (Figure 4A).

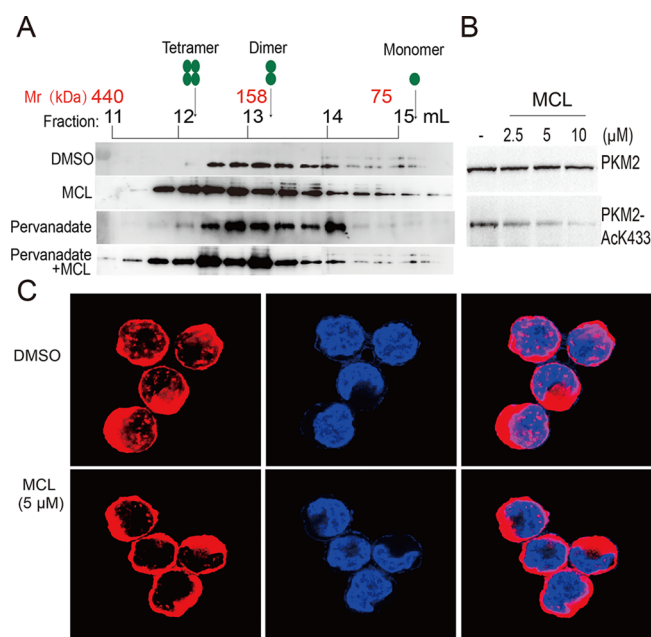


**Figure 4.** MCL promotes PKM2 tetramer formation and prevents AcK433 modification and nucleus translocation. (A) PKM2 subunit association was determined by Western blot using anti-PKM2 (Cell Signaling Technology, 4053) of the chromatographic fractions of HL60 cells treated with MCL, pervanadate, and MCL-combined pervanadate, lysed hypotonically, and analyzed by size-exclusion chromatography. Mr, relative molecular weight. (B) Effect of MCL on the AcK433 of PKM2. HL60 cells were preincubated with MCL (0, 2.5, 5, and 10 μM) for 20 h, followed by detection of endogenous PKM2 and AcK433 PKM2 by Western blot. (C) Subcellular localization of total PKM2 and MCL-treated PKM2 was examined by immunofluorescence microscopy in HL60 cells. HL60 cells were treated with MCL (5 μM) or DMSO for 20 h and reacted with anti-PKM2. After overnight incubation, the second antibody Alexa Fluor 647 conjugated goat antirabbit IgG (red) for PKM2 and Hoechst 33342 (blue) for nucleus were added to the image.

**MCL Decreases the K433 Acetylation of PKM2 and Reduces Its Nuclear Translocation.** Recently, Lv et al. reported that upon the stimulation of mitogenic and oncogenic signals, PKM2 was acetylated by p300 acetyltransferase at lysine433 (K433), which inactivates PKM2 by interfering with FBP binding and promotes the nuclear accumulation.<sup>20</sup> Dimer PKM2, when located at the nucleus, can function as a protein kinase and transcriptional coactivator to trigger the expression of genes that promote tumorigenesis and migration.<sup>8,20,21</sup> To explore the intracellular effect of MCL on PKM2, we incubated HL60 leukemia cells with DMSO or MCL and then extracted the cellular protein to detect the AcK433 modification of PKM2. Western blot developed with anti-AcK433-PKM2

indicated that AcK433 decreased with MCL treatment in a dose-dependent manner (Figure 4B, bottom). Meanwhile, Western blot developed with anti-PKM2 revealed that cellular PKM2 was present in comparable amounts among the different samples (Figure 4B, top). These data indicate that the MCL treatment has no effect on the protein level of PKM2 but reduces the acetylation at K433, contributing to the tetramerization of PKM2 indirectly. Interestingly, immunofluorescence analysis revealed that MCL treatment at 5 μM (note: most cells died at 10 μM, presumably as a result of nuclear damage) for 12 h resulted in retardation of the nuclear accumulation of PKM2 in HL60 cells (Figure 4C). Western blot analysis of subcellular fraction also confirmed the decrease of PKM2 in nuclear retardation (Figure S5). These results demonstrate that MCL is an effective PKM2 modulator, which inhibits both acetylation modification and nuclear translocation in cells, further suppressing the transcriptional regulation in tumorigenesis.

**Structural Analysis of the Binding Mode between MCL and PKM2.** To better understand the structure and regulatory properties of MCL binding to PKM2, we docked MCL into the human X-ray structure of PKM2 (PDB ID: 1T5A) using the docking package GOLD 5.1.<sup>22</sup> Each PKM2 monomer is composed of four domains: the N-terminal, A-, B-, and C-domains (Figure S6A–C), and can form oligomeric assemblies (dimers, tetramers, and, to a lesser extent, higher order oligomers). In order to mimic covalent binding, we defined two linking atoms, one from the MCL ligand (C13, Figure 1C) and the other from Cys424 (S), and forced them to occupy the same steric volume.

In the dimer formation, the subunit interface is formed by the adjacent C-domains (C–C' dimer interface, Figure S6A). In the tetramer formation, an additional interface is introduced between the neighboring A-domains (A–A' tetramer interface, Figure S6A). We first docked MCL moiety among the A-, C-, and N-terminal domains, and then performed extensive molecular dynamics (MD) simulations and molecular mechanics/generalized Born surface area continuum solvation (MM/GBSA) calculations to assess the stability of the tetramer or dimer with or without MCL binding. The relative flexibilities of the MCL-bound and MCL-free complexes were determined from the computed per residue B-factors. These values were calculated over the last 40 ns of the MD trajectories and subsequently mapped onto the PKM2 structures. Of the four PKM2 domains (A, B, C, and N-terminus), the B-domain experienced larger fluctuations during MD, while the A- and C-domains were less mobile, as these domains were involved in dimer and tetramer formation (Figure 5A). Moreover, in the MCL-bound state, the A-domain exhibited considerably less flexibility, and the N-terminal domain induced tetramer formation, which indicated that MCL binding can significantly stabilize the A–A' tetramer interface (Figure 5A). As for the interfacial binding energies of A–A' (tetramer formation) and C–C' (dimer formation), C–C' binding energies were little fluctuated, but A–A' binding energies were greatly enhanced by the addition of MCL, and the binding free energy  $\Delta G_b$  increased from  $-253.8 \text{ kcal}\cdot\text{mol}^{-1}$  (PKM2) to  $-322.3 \text{ kcal}\cdot\text{mol}^{-1}$  (PKM2:MCL complex) (Figure 5B). To identify the structural features responsible for stabilizing the A–A' and C–C' interfaces, we decomposed  $\Delta G_b$  into per residue contributions (1D MM/GBSA decomposition). Residue contributions were color mapped onto the structures of the respective interfaces (Figure S6D,E). In addition,  $\Delta G_{np}$  (or the

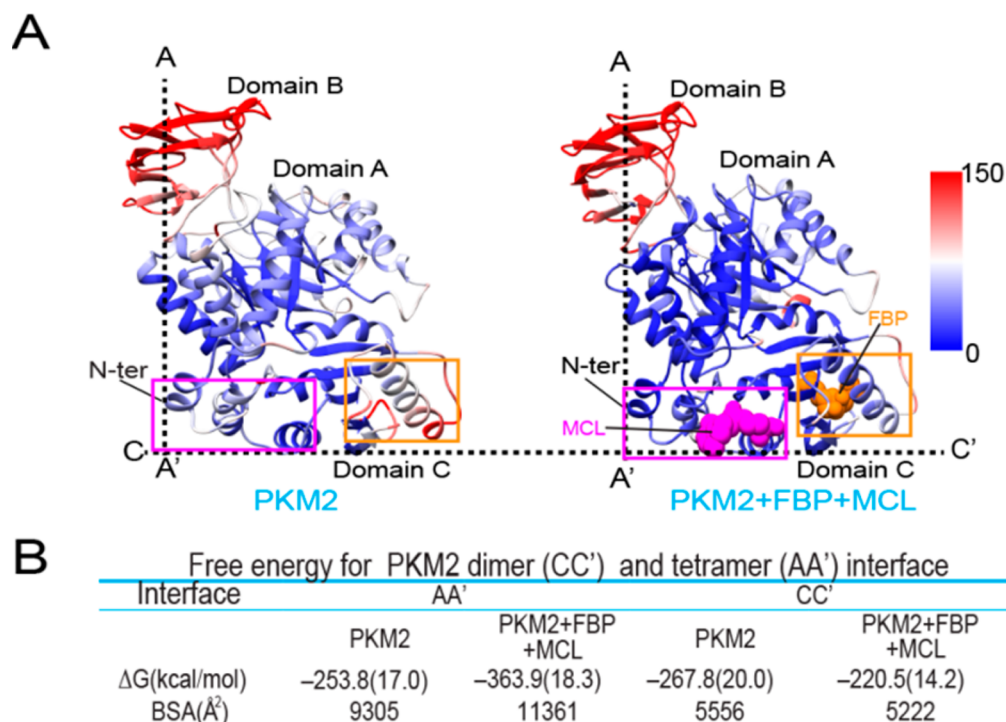


**Figure 5.** Activator MCL promotes PKM2 tetramer formation (PDB ID: 1ZJH and 1T5A; 1ZJH is the apo tetrameric PKM2 structure, and 1T5A is the FBP bound tetrameric PKM2 structure). (A) Computed B-factors mapped onto the PKM2 models highlight conformational differences. Coloring corresponds to computed B-factor values from high (red) to low (blue). (B) Computed free energy of AA' and CC' interface. Per residue binding energies computed from the 1D MM/GBSA decomposition. Residues are colored according to the value of the binding energy in kcal/mol from red (positive) to blue (negative). The bound MCL are shown as magenta spheres. The large (AA') and small (CC') interfaces between monomers are presented as dashed lines. Only one monomer is shown.

buried surface area, BSA) correlated well with the overall binding energies, indicating that MCL promoted tetramer formation by increasing the BSA at the tetramer interface. Overall, these data suggest that new interactions at A–A' interface with MCL binding appear to be directly responsible for the observed increase in binding free energy and stabilization of the PKM2 tetramers. In contrast, TEPP-46 was found in the A–A' interface and interacts with the surrounding residues Asp354, Ala388, Tyr390, and Leu394 through polar and van der Waals interactions. The binding residues and interaction energy of TEPP-46 are quite different from that of MCL.

**Anticancer Activity of MCL Is Dependent on the Expression of PKM2.** To investigate the influence of PKM2 on the MCL-mediated inhibition of leukemia cell viability, we knock down the expression of PKM2 in HL60 cells by lentiviral delivery of specific short hairpin RNA for PKM2 (*shPKM2*) or mock (*shControl*). Western blot showed that *shPKM2* inhibited the expression of PKM2 but not PKM1 (Figure 6A), indicating the specificity of *shPKM2*. Concomitantly, stable knockdown of PKM2 resulted in decreased pyruvate kinase activity of PKM2 (69% of *shControl*) and reduced cell viability (83% of *shControl*) (Figure 6B,C). These data were consistent to the results of Goldberg et al. in which cell viability was drastically reduced among 10 cancer cell lines with the treatment of *shPKM2*.<sup>23</sup> Then *shPKM2* and *shControl* cells were treated with MCL or DMSO for 24 h, and the cell viability was assayed. Results indicate that the *shPKM2* cells are less sensitive to the inhibitory effect of MCL than *shControl* cells (Figure 6D), implying the effect of MCL on cancer cell viability is mainly dependent on PKM2.

### Evaluation of the Inhibitive Effect of DMAMCL in Xenograft Zebrafish.

To assess the anticancer effects of DMAMCL, xenograft zebrafishes were established via injection of human leukemia HL60 cells in zebrafish embryos. HL60 cells were first stained with cell tracker CM-Dil (red fluorescence color) and then transplanted into zebrafish embryos at 2 days postfertilization (2dpf). Following transplantation, nine injected zebrafish groups were treated with drugs at different dosages over the course of 3 days. Compared with the control group, 80% zebrafish died when the dosage of DMAMCL exceeded 20  $\mu\text{g/mL}$ , whereas the survival rate approached 100% at a concentration of 10  $\mu\text{g/mL}$  or lower. Notably, with dosages between 1–10  $\mu\text{g/mL}$ , DMAMCL produced a dose-dependent decrease in cell dissemination (Figure 6E) with respect to both proliferation and migration. Results of this study indicated that optimal inhibition of dissemination was observed with DMAMCL treatment at a dose of 10  $\mu\text{g/mL}$ , with proliferation and migration inhibition rates of 56.44% ( $P < 0.01$ ) and 58.10% ( $P < 0.01$ ), which exceeded rates following cytarabine treatment (200  $\mu\text{g/mL}$ ) of 43.28% ( $P < 0.01$ ) and 44.04% ( $P < 0.01$ ) (Tables S1 and S2).

These data demonstrate that the activation of PKM2 by MCL results in significant suppression of tumor growth *in vivo*, indicating DMAMCL acts as a novel PKM2 activator with promising potential for anticancer therapeutics.

### CONCLUSIONS

Targeting tumor-specific metabolic pathways is a novel strategy for cancer therapy.<sup>1</sup> Recent studies have identified that PKM2 is abundantly expressed in AML cell lines and primary AML patient samples.<sup>24–26</sup> Combined with the up-regulation in other



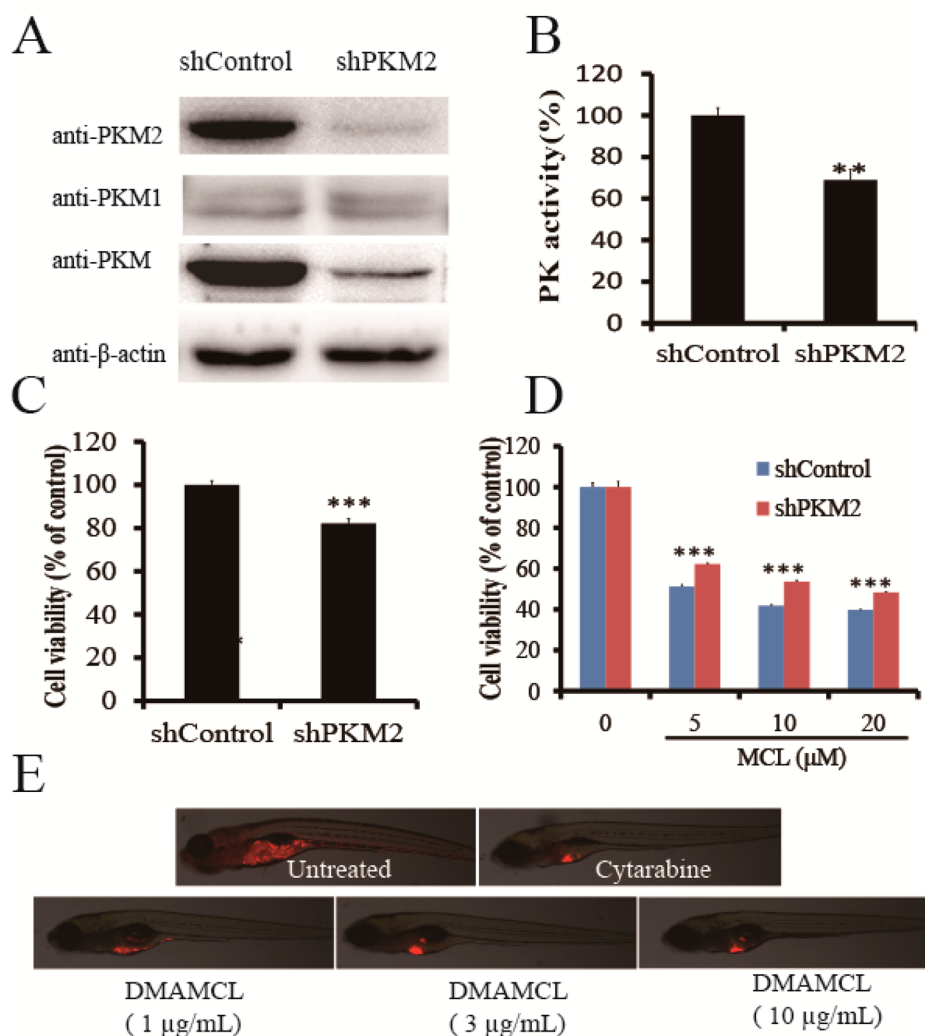


**Figure 6.** Anticancer effects of DMAMCL are dependent on PKM2. (A) Western blot detection of the expression of PKM1, PKM2, and PKM in the absence of endogenous PKM2, which was knocked down with short hairpin RNA. (B) Cell-based detection of pyruvate activity of HL60 cells with *shPKM2* and *shControl*. (C) Cell viability detection of pyruvate activity of HL60 cells with *shPKM2* and *shControl*. (D) PKM2 depletion desensitizes cancer cells to MCL treatment. (E) Representative fluorescent images of HL60 cell xenografted zebrafishes with treatment of DMAMCL, cytarabine, or negative control. Approximately 300 HL60 cells were injected into the yolk sac of embryos. After injections, xenografted embryos were treated with a series of doses of DMAMCL (1, 3, 10  $\mu\text{g}/\text{mL}$ ), cytarabine at 200  $\mu\text{g}/\text{mL}$  as a positive drug control, and saline as a negative control. After 3 days of incubation, the number of embryos exhibiting cancer cell dissemination was counted by microscopic observation (15 larvae/group). Data represent the average  $\pm$  SD of three independent assays. \* $P < 0.05$ . \*\* $P < 0.01$ .

cancer cells, PKM2 has been identified as a promising potential target for cancer therapy.<sup>3</sup> However, PKM2 knockdown in HCT116 and RKO colon cancer cells demonstrated that the growth of xenograft tumors is unaffected *in vivo*.<sup>27</sup> Moreover, PKM2 knockdown accelerates tumor formation in a Brcal-loss-driven mice model of breast cancer.<sup>5</sup> In contrast, the genetic replacement of PKM2 with active PKM1 decreased the proliferation of cancer cells *in vitro* and suppressed the formation of cancer cell xenograft tumors in mice.<sup>1,9</sup> Thus, low pyruvate activity caused by an inactive state of PKM2 (dimer) is the key for the proliferation of cancer cells within tumors.<sup>5</sup> Fixation PKM2 in its active tetrameric form by activators is anticipated to be a novel treatment for cancer therapy.<sup>3,9,10</sup>

MCL, a natural guaianolide sesquiterpene lactone, which was discovered in *Michelia compressa* and *Michelia champaca* plants, has been shown to exert potent anticancer properties on AML and glioma cells.<sup>15,16</sup> The present study demonstrated

that DMAMCL inhibited several cancer cells growth *in vitro* and repressed tumor growth in leukemia HL60 xenografted zebrafish. To determine the specific target of MCL, we analyzed the SAR of MCL and synthesized both a positive (3) and negative (4) probe. Using this pair of probes, we found that MCL selectively targeted PKM2 but not PKM1 in HL-60 cells. Through LC-MS/MS analysis and a PKM2 activity assay, we found that MCL selectively binds to the conserved C424 residue of PKM2, promoting tetramer formation and elevating pyruvate activity. These promising results indicate that activation of PKM2 via natural product compound might be a useful anticancer strategy in the clinic.

Interestingly, recent advances reported that various stimuli and post-translational modifications can trigger PKM2 translocation into nucleus.<sup>17,20,28,29</sup> Once accumulated in the nucleus, PKM2 functions as coactivator or protein kinase to promote tumor growth or proliferation.<sup>7,8,21,30,31</sup> In this study, we found that MCL inhibited the K433 acetylation of PKM2

but not the protein level. Meanwhile, the nuclear PKM2 was reduced concomitantly, which will block its signaling role for proliferation. To our knowledge, MCL is the first known or reported covalently bound, natural-product-derived PKM2 modulator, which interferes with the role of PKM2 both in cytoplasm and nucleus.

PKM2 integrates metabolic inputs and nuclear signaling in tumorigenesis, and has been investigated as a novel target for cancer therapy. Data reported in this study argue that MCL, the active drug derived from DMAMCL, enhances PKM2 activity by stably promoting the more active tetrameric formation and reduces its nuclear translocation, which will unveil the mechanism of DMAMCL and inform clinical trials for cancer treatment.

## ■ EXPERIMENTAL SECTION

**Reagents and General Synthetic Procedures.** Reagents were purchased at the highest commercial quality and used without further purification, unless otherwise stated. NMR spectra were recorded with a 400 MHz ( $^1\text{H}$ , 400 MHz;  $^{13}\text{C}$ , 100 MHz) spectrometer and referenced to the solvent peak for  $\text{CDCl}_3$ . Synthesis and chemical confirmation of micheliolide (MCL), S-MCL, DMAMCL, biotin-S-MCL, and biotin-MCL are described in [SI Materials and Methods](#). The purity of these compounds was confirmed to be  $\geq 95\%$  by analytical HPLC with an ODS-C18 column ( $4.6 \times 150$  mm,  $5 \mu\text{m}$ ) eluted at 1 mL/min with Milli-Q water and  $\text{CH}_3\text{CN}$ . Antibodies and other reagents used in this study were purchased directly from the vendors listed in [SI Materials and Methods](#).

**Cell Lines and Culture.** HL-60, KG-1a, K562, HL-60/ADR, KG-1a/ADR, K562/ADR, SW1990, and SH-SY5Y were purchased from ATCC and authenticated by short tandem repeat testing. All the cell lines were maintained in appropriate medium as the manufacturer suggested. HL-60, KG-1a, K562, HL-60/ADR, KG-1a/ADR, and K562/ADR were cultured in RPMI 1640 medium (Sigma-Aldrich, St. Louis, MO, USA) supplemented with 12% fetal bovine serum (FBS; Gibco BRL, Gaithersburg, MD, USA), penicillin (100 IU/mL), and streptomycin (100  $\mu\text{g}/\text{mL}$ ) in a humidified incubator at  $37^\circ\text{C}$  and 5%  $\text{CO}_2/95\%$  air. Prior to each experiment, HL-60/ADR, KG-1a/ADR, and K562/ADR cells were treated with 1  $\mu\text{mol}/\text{mL}$  ADR (Sigma-Aldrich, St. Louis, MO, USA) for 10–28 days and then cultured for 10 days without ADR exposure. SW1990 and SH-SY5Y were cultured in DMEM medium (Sigma-Aldrich, St. Louis, MO, USA) supplemented with 10% fetal bovine serum (FBS; Gibco BRL, Gaithersburg, MD, USA), penicillin (100 IU/mL), and streptomycin (100  $\mu\text{g}/\text{mL}$ ). All the cell lines were tested for mycoplasma contamination and were found to be negative.

For experiments, cells were treated with compounds for different concentrations with 0.1% dimethyl sulfoxide (DMSO; Sigma-Aldrich, St. Louis, MO, USA) as solvent control. Where indicated, 100  $\mu\text{M}$  pervanadate was added 10 min before cell lysis.

**Plasmids, shRNA Virus Production, and Infection.** Expression plasmids for human PKM1 and PKM2, pET28a-PKM1 and pET28a-PKM2 plasmids, were donated by Dr. Zhiren Liu's group. To get cysteine424 mutated PKM2 plasmid, site-directed mutant was constructed using QuikChange II XL Site-Directed Mutagenesis Kit (Stratagene, USA) and primers (forward, 5'-attatggccccactggagcacttg-aaggagg-3'; reverse, 5'-cctcctcaagtgtcctcagtgggccataat-3'). After confirming a 100% identities match by DNA sequencing (Invitrogen, Shanghai, China), the *E. coli* strain BL21 was transformed with constructs for the next step of protein purification.

The shRNAs targeting the sequence of human PKM2 (corresponding to exon 10 of the human PKM) and corresponding negative control (NC) were designed as previous reported.<sup>23</sup> The shRNA for PKM2 was 5'-CCATAATCGTCCTCACCAA-3'; the shRNA for negative control was 5'-CUUACGCUGAGUACUUCGA-3'. The recombinant lentivirus containing *shPKM2* or *shControl* was packaged using hU6-MCS-Ubiquitin-EGFP-IRES-puromycin lenti-viral vector provided by Shanghai GeneChem (China). HL60 was infected by

adding the lentiviral particles to the culture with 5  $\mu\text{g}/\text{mL}$  Polybrene. For generating stable cell lines, infected cells were selected with 1  $\mu\text{g}/\text{mL}$  puromycin (Sigma) for 72 h.

**Cell-Based Pyruvate Kinase Activity Assay.** HL60 or HL60-shPKM2 leukemia cells were plated at  $2 \times 10^5$  cells per well (six-well plate) in RPMI 1640 media plus 12% FBS. Pervanadate (100  $\mu\text{M}$ ) was added 10 min prior to cell lysis.<sup>9</sup> Then, cells were lysed on ice with NP-40 buffer containing 2 mM DTT and protease inhibitors for about 30 min and clarified by centrifugation at  $14,000g$  for 5 min. The PK activity in lysates was determined by Pyruvate Kinase Activity Assay (Sigma, MAK072-1KT).<sup>32</sup>

**In Vivo Tumor Models.** All animal studies were conducted according to protocols approved by the Animal Ethics Committee of Nankai University, in accordance with Principles of Laboratory Animal Care and Use Programs. Zebrafish (albino) were obtained from the Zebrafish International Resource Center (Eugene, Oregon, USA) and housed in an automated fish housing system (Hunter Biotechnology Inc., China) at  $28^\circ\text{C}$ . Care and treatment of zebrafish were conducted in accordance with guidelines approved by the Association for Assessment and Accreditation of Laboratory Animal Care (AAALAC).

**Statistical Analysis.** Kaplan–Meier survival analysis (SPSS 10.0; SPSS, Inc.) was used to compare drug-treated versus control animals. An unpaired Student's *t* test was used to evaluate the difference between two different treatments, where a *P* value of less than 0.05 was considered statistically significant. Statistical analyses were performed using PRISM software (Irvine, CA, USA).

## ■ ASSOCIATED CONTENT

### § Supporting Information

The Supporting Information is available free of charge on the ACS Publications website at DOI: [10.1021/acs.jmedchem.8b00241](https://doi.org/10.1021/acs.jmedchem.8b00241).

Supplementary figures and tables, methods for chemical synthesis, MTT assay for DMAMCL, pull-down of biotin-MCL bound proteins, molecular modeling, Western blot, immunofluorescence analysis, preparation of recombinant proteins, gel filtration of cell fraction, recombinant PKM2 activity assay, protein identification by LC–MS/MS, kinetic determination of PKM2-MCL interaction, and anticancer evaluation in HL60 cells xenografted zebrafish ([PDF](#))

Molecular formula strings ([CSV](#))

Apo tetrameric PKM2 structure (PDB ID: 1ZJH) ([PDB](#))

FBP bound tetrameric PKM2 structure (PDB ID: 1T5A) ([PDB](#))

### Accession Codes

Docked models of 1 into the FBP bound tetrameric PKM2 structure (PDB ID: 1T5A) and apo tetrameric PKM2 structure (PDB ID: 1ZJH) are shown in [Figures 5](#) and [S6](#).

## ■ AUTHOR INFORMATION

### Corresponding Authors

\*E-mail: [yuechen@nankai.edu.cn](mailto:yuechen@nankai.edu.cn).

\*E-mail: [pwang11@gsu.edu](mailto:pwang11@gsu.edu).

### ORCID

Jing Li: [0000-0002-4289-4829](https://orcid.org/0000-0002-4289-4829)

Cheng Ma: [0000-0002-0017-2182](https://orcid.org/0000-0002-0017-2182)

Ivaylo Ivanov: [0000-0002-5306-1005](https://orcid.org/0000-0002-5306-1005)

Peng George Wang: [0000-0003-3335-6794](https://orcid.org/0000-0003-3335-6794)

Yue Chen: [0000-0002-1317-7097](https://orcid.org/0000-0002-1317-7097)

### Notes

The authors declare no competing financial interest.



## ACKNOWLEDGMENTS

We thank Qunying Lei for kindly providing antibody for K433 acetylation of PKM2. We also thank Jenny Yang, Zhiren Liu, and Binghe Wang of Georgia State University for their help in instruction of experiments. This work was supported, in part, by grants from the National Science Fund for Distinguished Young Scholars of China (No. 81625021), the National Institutes of Health (U01GM116263 and GM110387), the National Science Foundation of China (No. 31000371), the International Science & Technology Cooperation Program of China (No. 2015DFR40460), and the Natural Science Foundation of Tianjin (15JCYBJC29000). Computational resources were provided in part by a National Science Foundation XSEDE allocation (CHE110042) and by the National Energy Research Scientific Computing Center (NERSC) supported by the U.S. Department of Energy Office of Science (DE-AC02-05CH11231).

## ABBREVIATIONS USED

MCL, micheliolide; S-MCL, single bond MCL; biotin-MCL, biotin conjugated micheliolide; biotin-S-MCL, biotin conjugated single bond micheliolide; PKM2, pyruvate kinase M2; PKM1, pyruvate kinase M1; PEP, phosphoenol-pyruvate; SLs, sesquiterpene lactones; PTL, parthenolide; GSL, guaianolide sesquiterpene lactone; AML, acute myelogenous leukemia; DMAMCL, dimethylaminomicheliolide; MTT, 3-[4,5-dimethylthiazol-2-yl]-2,5-diphenyl tetrazolium; SAR, structure-activity relationship; rPKM1, recombinant PKM1; rPKM2, recombinant PKM2;  $AC_{50}$ , half-maximum activating concentration; pTyr, phosphotyrosine; MD, molecular dynamics;  $K_{obs}$ , observed rate constants for binding;  $K_i$ , apparent dissociation constant for the initial PKM2:biotin-MCL complex; MM/GBSA, molecular mechanics/generalized Born surface area continuum salvation; *sh*PKM2, specific short hairpin RNA for gene PKM2; *sh*Control, specific short hairpin RNA mock; 2dpf, two days postfertilization; AAALAC, Assessment and Accreditation of Laboratory Animal Care; PME, particle mesh Ewald; MM/GBSA, generalized Born and surface area continuum salvation; IPTG, isopropyl  $\beta$ -D-1-thiogalactopyranoside

## REFERENCES

- (1) Christofk, H. R.; Vander Heiden, M. G.; Harris, M. H.; Ramanathan, A.; Gerszten, R. E.; Wei, R.; Fleming, M. D.; Schreiber, S. L.; Cantley, L. C. The M2 splice isoform of pyruvate kinase is important for cancer metabolism and tumour growth. *Nature* **2008**, *452*, 230–233.
- (2) Chaneton, B.; Hillmann, P.; Zheng, L.; Martin, A. C.; Maddocks, O. D.; Chokkathukalam, A.; Coyle, J. E.; Jankevics, A.; Holding, F. P.; Vousden, K. H.; Frezza, C.; O'Reilly, M.; Gottlieb, E. Serine is a natural ligand and allosteric activator of pyruvate kinase M2. *Nature* **2012**, *491*, 458–462.
- (3) Dayton, T. L.; Jacks, T.; Vander Heiden, M. G. PKM2, cancer metabolism, and the road ahead. *EMBO Rep.* **2016**, *17*, 1721–1730.
- (4) Keller, K. E.; Tan, I. S.; Lee, Y. S. SAICAR stimulates pyruvate kinase isoform M2 and promotes cancer cell survival in glucose-limited conditions. *Science* **2012**, *338*, 1069–1072.
- (5) Israelsen, W. J.; Dayton, T. L.; Davidson, S. M.; Fiske, B. P.; Hosios, A. M.; Bellinger, G.; Li, J.; Yu, Y.; Sasaki, M.; Horner, J. W.; Burga, L. N.; Xie, J.; Jurczak, M. J.; DePinho, R. A.; Clish, C. B.; Jacks, T.; Kibbey, R. G.; Wulf, G. M.; Di Vizio, D.; Mills, G. B.; Cantley, L. C.; Vander Heiden, M. G. PKM2 isoform-specific deletion reveals a differential requirement for pyruvate kinase in tumor cells. *Cell* **2013**, *155*, 397–409.
- (6) Azoitei, N.; Becher, A.; Steinestel, K.; Rouhi, A.; Diepold, K.; Genze, F.; Simmet, T.; Seufferlein, T. PKM2 promotes tumor angiogenesis by regulating HIF-1 $\alpha$  through NF- $\kappa$ B activation. *Mol. Cancer* **2016**, *15*, 3–3.
- (7) Gao, X.; Wang, H.; Yang, J. J.; Liu, X.; Liu, Z. R. Pyruvate kinase M2 regulates gene transcription by acting as a protein kinase. *Mol. Cell* **2012**, *45*, 598–609.
- (8) Yang, W.; Xia, Y.; Hawke, D.; Li, X.; Liang, J.; Xing, D.; Aldape, K.; Hunter, T.; Alfred Yung, W. K.; Lu, Z. PKM2 phosphorylates histone H3 and promotes gene transcription and tumorigenesis. *Cell* **2012**, *150*, 685–696.
- (9) Anastasiou, D.; Yu, Y.; Israelsen, W. J.; Jiang, J. K.; Boxer, M. B.; Hong, B. S.; Tempel, W.; Dimov, S.; Shen, M.; Jha, A.; Yang, H.; Mattaini, K. R.; Metallo, C. M.; Fiske, B. P.; Courtney, K. D.; Malstrom, S.; Khan, T. M.; Kung, C.; Skoumbourdis, A. P.; Veith, H.; Southall, N.; Walsh, M. J.; Brimacombe, K. R.; Leister, W.; Lunt, S. Y.; Johnson, Z. R.; Yen, K. E.; Kunii, K.; Davidson, S. M.; Christofk, H. R.; Austin, C. P.; Inglese, J.; Harris, M. H.; Asara, J. M.; Stephanopoulos, G.; Salituro, F. G.; Jin, S.; Dang, L.; Auld, D. S.; Park, H. W.; Cantley, L. C.; Thomas, C. J.; Vander Heiden, M. G. Pyruvate kinase M2 activators promote tetramer formation and suppress tumorigenesis. *Nat. Chem. Biol.* **2012**, *8*, 839–847.
- (10) DeLaBarre, B.; Hurov, J.; Cianchetta, G.; Murray, S.; Dang, L. Action at a distance: allostery and the development of drugs to target cancer cell metabolism. *Chem. Biol.* **2014**, *21*, 1143–1161.
- (11) Mann, J. Natural products in cancer chemotherapy: past, present and future. *Nat. Rev. Cancer* **2002**, *2*, 143–148.
- (12) Guzman, M. L.; Rossi, R. M.; Karnischky, L.; Li, X.; Peterson, D. R.; Howard, D. S.; Jordan, C. T. The sesquiterpene lactone parthenolide induces apoptosis of human acute myelogenous leukemia stem and progenitor cells. *Blood* **2005**, *105*, 4163–4169.
- (13) Wiedhopf, R. M.; Young, M.; Bianchi, E.; Cole, J. R. Tumor inhibitory agent from *Magnolia grandiflora* (Magnoliaceae). I. Parthenolide. *J. Pharm. Sci.* **1973**, *62*, 345–345.
- (14) Jin, P.; Madieh, S.; Augsburger, L. L. The solution and solid state stability and excipient compatibility of parthenolide in feverfew. *AAPS PharmSciTech* **2007**, *8*, E105.
- (15) An, Y.; Guo, W.; Li, L.; Xu, C.; Yang, D.; Wang, S.; Lu, Y.; Zhang, Q.; Zhai, J.; Fan, H.; Qiu, C.; Qi, J.; Chen, Y.; Yuan, S. Micheliolide derivative DMAMCL inhibits glioma cell growth *in vitro* and *in vivo*. *PLoS One* **2015**, *10*, e0116202.
- (16) Zhang, Q.; Lu, Y.; Ding, Y.; Zhai, J.; Ji, Q.; Ma, W.; Yang, M.; Fan, H.; Long, J.; Tong, Z. Guaianolide sesquiterpene lactones, a source to discover agents that selectively inhibit acute myelogenous leukemia stem and progenitor cells. *J. Med. Chem.* **2012**, *55*, 8757–8769.
- (17) Anastasiou, D.; Poulogiannis, G.; Asara, J. M.; Boxer, M. B.; Jiang, J. K.; Shen, M.; Bellinger, G.; Sasaki, A. T.; Locasale, J. W.; Auld, D. S.; Thomas, C. J.; Vander Heiden, M. G.; Cantley, L. C. Inhibition of pyruvate kinase M2 by reactive oxygen species contributes to cellular antioxidant responses. *Science* **2011**, *334*, 1278–1283.
- (18) Ahn, K.; Johnson, D. S.; Mileni, M.; Beidler, D.; Long, J. Z.; McKinney, M. K.; Weerapana, E.; Sadagopan, N.; Liimatta, M.; Smith, S. E.; Lazerwith, S.; Stiff, C.; Kamtekar, S.; Bhattacharya, K.; Zhang, Y.; Swaney, S.; Van Becelaere, K.; Stevens, R. C.; Cravatt, B. F. Discovery and characterization of a highly selective FAAH inhibitor that reduces inflammatory pain. *Chem. Biol.* **2009**, *16*, 411–420.
- (19) Christofk, H. R.; Vander Heiden, M. G.; Wu, N.; Asara, J. M.; Cantley, L. C. Pyruvate kinase M2 is a phosphotyrosine-binding protein. *Nature* **2008**, *452*, 181–186.
- (20) Lv, L.; Xu, Y. P.; Zhao, D.; Li, F. L.; Wang, W.; Sasaki, N.; Jiang, Y.; Zhou, X.; Li, T. T.; Guan, K. L.; Lei, Q. Y.; Xiong, Y. Mitogenic and oncogenic stimulation of K433 acetylation promotes PKM2 protein kinase activity and nuclear localization. *Mol. Cell* **2013**, *52*, 340–352.
- (21) Yang, W.; Xia, Y.; Ji, H.; Zheng, Y.; Liang, J.; Huang, W.; Gao, X.; Aldape, K.; Lu, Z. Nuclear PKM2 regulates beta-catenin transactivation upon EGFR activation. *Nature* **2011**, *478*, 118–122.

(22) Jones, G.; Willett, P.; Glen, R. C.; Leach, A. R.; Taylor, R. Development and validation of a genetic algorithm for flexible docking. *J. Mol. Biol.* **1997**, *267*, 727–748.

(23) Goldberg, M. S.; Sharp, P. A. Pyruvate kinase M2-specific siRNA induces apoptosis and tumor regression. *J. Exp. Med.* **2012**, *209*, 217–224.

(24) Guzman, M. L. Cytokine induced nuclear localization of pyruvate kinase M2 in acute myeloid leukemia. *Blood* **2013**, *122*, 5406–5406.

(25) Hulleman, E.; Broekhuis, M. J.; Pieters, R.; Den Boer, M. L. Pyruvate kinase M2 and prednisolone resistance in acute lymphoblastic leukemia. *Haematologica* **2009**, *94*, 1322–1324.

(26) Wang, Y. H.; Israelsen, W. J.; Lee, D.; Yu, V. W.; Jeanson, N. T.; Clish, C. B.; Cantley, L. C.; Vander Heiden, M. G.; Scadden, D. T. Cell-state-specific metabolic dependency in hematopoiesis and leukemogenesis. *Cell* **2014**, *158*, 1309–1323.

(27) Cortés-Cros, M.; Hemmerlin, C.; Ferretti, S.; Zhang, J.; Gounarides, J. S.; Yin, H.; Muller, A.; Haberkorn, A.; Chene, P.; Sellers, W. R. M2 isoform of pyruvate kinase is dispensable for tumor maintenance and growth. *Proc. Natl. Acad. Sci. U. S. A.* **2013**, *110*, 489–494.

(28) Wang, Y.; Liu, J.; Jin, X.; Zhang, D.; Li, D.; Hao, F.; Feng, Y.; Gu, S.; Meng, F.; Tian, M.; Zheng, Y.; Xin, L.; Zhang, X.; Han, X.; Aravind, L.; Wei, M. O-GlcNAcylation destabilizes the active tetrameric PKM2 to promote the Warburg effect. *Proc. Natl. Acad. Sci. U. S. A.* **2017**, *114*, 13732–13737.

(29) Liu, F.; Ma, F.; Wang, Y.; Hao, L.; Zeng, H.; Jia, C.; Wang, Y.; Liu, P.; Ong, I. M.; Li, B.; Chen, G.; Jiang, J.; Gong, S.; Li, L.; Xu, W. PKM2 methylation by CARM1 activates aerobic glycolysis to promote tumorigenesis. *Nat. Cell Biol.* **2017**, *19*, 1358–1370.

(30) Jiang, Y.; Wang, Y.; Wang, T.; Hawke, D. H.; Zheng, Y.; Li, X.; Zhou, Q.; Majumder, S.; Bi, E.; Liu, D. X.; Huang, S.; Lu, Z. PKM2 phosphorylates MLC2 and regulates cytokinesis of tumour cells. *Nat. Commun.* **2014**, *5*, 5566–5566.

(31) Luo, W.; Hu, H.; Chang, R.; Zhong, J.; Knabel, M.; O'Meally, R.; Cole, R. N.; Pandey, A.; Semenza, G. L. Pyruvate kinase M2 is a PHD3-stimulated coactivator for hypoxia-inducible factor 1. *Cell* **2011**, *145*, 732–744.

(32) Parnell, K. M.; Foulks, J. M.; Nix, R. N.; Clifford, A.; Bullough, J.; Luo, B.; Senina, A.; Vollmer, D.; Liu, J.; McCarthy, V.; Xu, Y.; Saunders, M.; Liu, X. H.; Pearce, S.; Wright, K.; O'Reilly, M.; McCullar, M. V.; Ho, K. K.; Kanner, S. B. Pharmacologic activation of PKM2 slows lung tumor xenograft growth. *Mol. Cancer Ther.* **2013**, *12*, 1453–1460.